CHAPTER 2

Climate change

James W. Hurrell[1] and Kevin E. Trenberth

2.1 Introduction

Global climate change is significantly altering the structure and functioning of many ecosystems and, consequently, temporal and spatial patterns of population and species abundance (e.g. Stenseth *et al*., 2005; Rosenzweig *et al*., 2008). Significant advances in the scientific understanding of climate change now make it clear that there has been a change in climate that goes beyond the range of natural variability. As stated in the Fourth Assessment Report (AR4) of the Intergovernmental Panel on Climate Change (IPCC), the warming of the climate system is 'unequivocal' and it is 'very likely due to human activities'. The culprit is the astonishing rate at which greenhouse gas (GHG) concentrations are increasing in the atmosphere, mostly through the burning of fossil fuels and changes in land use, such as those associated with agriculture and deforestation. GHGs are relatively transparent to incoming solar radiation while they absorb and reemit outgoing infrared radiation. The result is that more energy stays in the global climate system, not only raising temperature but also producing many other direct and indirect changes in the climate system.

The indisputable evidence of anthropogenic climate change, and the knowledge that global climate change will continue well into the future under any plausible emission scenario, is now a factor in the planning of many organizations and governments. Global warming does not imply, however, that future changes in weather and climate will be uniform around the globe. The land, for instance, is warming faster than the oceans, consistent with its smaller heat capacity. Moreover, uncertainties remain regarding how climate will change at regional and local scales where the signal of natural variability is large, especially over the next several decades (Hawkins and Sutton, 2009). Regional differences in land and ocean temperatures arise, for instance, from natural variability such as El Niño Southern Oscillation (ENSO) events. Natural variability can result from purely internal atmospheric processes as well as from interactions among the different components of the climate system, such as those between the atmosphere and ocean, or the atmosphere and land.

El Niño events produce very strong warming of the central and eastern tropical Pacific Ocean, while the ocean cools over portions of the subtropics and the tropical western Pacific. Over the Atlantic, average basin-wide warming is imposed on top of strong, natural variability on multi-decadal time scales, called the Atlantic multi-decadal oscillation (AMO). The level of natural variability, in contrast, is relatively small over the tropical Indian Ocean, where surface warming has been steady and large over recent decades. Importantly, these differences in regional rates of sea surface

[1] The National Center for Atmospheric Research is sponsored by the National Science Foundation. Any opinions, findings, and conclusions or recommendations expressed in this publication are those of the authors and do not necessarily reflect the views of the National Science Foundation.

temperature (SST) change perturb the atmospheric circulation and shift storm tracks, so that some land regions become warmer and drier, while other regions cool as they become wetter. It is clear, therefore, that on the regional scales on which most planning decisions are made and impacts felt, future warming will not be smooth. Instead, it will be strongly modulated by natural climate variations, and especially those driven by the slowly varying oceans on a time scale of decades. This non-uniformity of change highlights the challenges of regional climate change that has considerable spatial structure and temporal variability.

It is the purpose of this chapter to review observed changes in climate, with a focus on changes in surface climate and on the atmospheric circulation, including variations in major modes of climate variability. However, the next section will first describe how natural and anthropogenic drivers of climate change are assessed using climate models. The chapter concludes with a brief summary of future-projected changes in climate. The physical evidence and the impacts on the environment and society, as documented in the AR4 (IPCC, 2007a,b), provide the main basis and reference for the chapter, although the material is updated where appropriate.

2.2 Human and natural drivers of climate change

The AR4 of IPCC (2007a) concluded that most of the observed global temperature increase of the past 50 years (Figure 2.1) is 'very likely'[2] due to human activity, while anthropogenic forcing has 'likely' contributed to changes in wind patterns, affecting extratropical storm tracks and regional temperature patterns in both the Northern and the Southern Hemispheres (NH and SH). These conclusions are based on studies that assess the causes of climate change, taking into account all possible agents of climate change (forcings), both natural and from human activities.

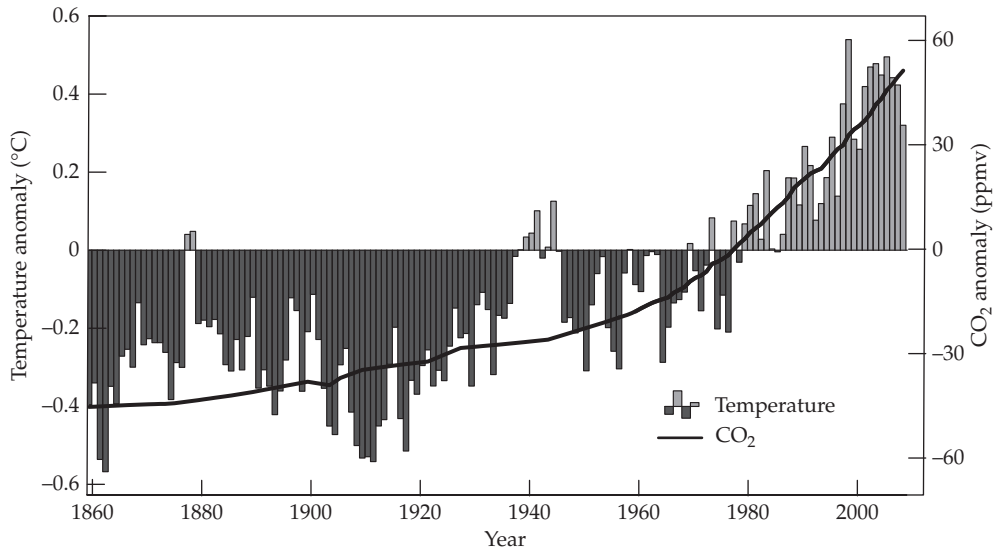

Figure 2.1 Estimated changes in annual global mean surface temperatures (°C, bars) and CO_2 concentrations (thick black line) over the past 149 years relative to 1961–1990 average values. Carbon dioxide concentrations since 1957 are from direct measurements at Mauna Loa, Hawaii, while earlier estimates are derived from ice core records. The scale for CO_2 concentrations is in parts per million (ppm) by volume, relative to a mean of 333.7 ppm, while the temperature anomalies are relative to a mean of 14°C. Updated from Trenberth (1997); see also Hurrell (2002) and Karl and Trenberth (2003).

[2] The IPCC AR4 defines the term 'very likely' as the likelihood of a result exceeding 90%, and the term 'likely' as exceeding 66%.

Note that forcings are external to the climate system and may arise, for instance, from changes in the sun or from changes in atmospheric composition associated with explosive volcanic eruptions. These phenomena occur naturally. Human activities that generate heat or change the atmospheric composition are also external to the climate system but do not occur naturally. In contrast, many feedbacks occur through interactions among the components of the climate system: the atmosphere, ocean, land, and cryosphere. Some amplify the original changes, producing a positive feedback, while others diminish them, giving a negative feedback. Feedbacks considerably complicate the climate system, and the physical processes involved are depicted in climate models. Radiative forcing is a measure of the influence that a factor has in altering the balance of incoming and outgoing energy in the Earth–atmosphere system and is an index of the importance of the factor as a potential climate change mechanism. Positive forcing tends to warm the surface while negative forcing tends to cool it.

The capability of climate models to simulate the past climate is comprehensively assessed by IPCC. Given good replications of the past, the forcings can be inserted one by one to disassemble their effects and allow attribution of the observed climate change to different forcings. Climate models therefore are a key tool to evaluate the role of various forcings in producing the observed changes in temperature and other climate variables.

The best climate models encapsulate the current understanding of the physical processes involved in the climate system, the interactions, and the performance of the system as a whole. Uncertainties arise, however, from shortcomings in the understanding and how to best represent complex processes in models. Yet, in spite of these uncertainties, today's best climate models are able to reproduce the climate of the past century, and simulations of the evolution of global surface temperature over the past millennium are consistent with paleoclimate reconstructions (IPCC, 2007a).

As a result, climate modellers are able to test the role of various forcings in producing observed changes in climate. Human activities increase GHGs, such as carbon dioxide (CO_2), methane (CH_4), nitrous oxide (N_2O) and other traces gases. They also increase aerosol concentrations in the atmosphere, mainly through the injection of sulphur dioxide (SO_2) from power stations and through biomass burning. A direct effect of sulphate aerosols is the reflection of a fraction of solar radiation back to space, which tends to cool the Earth's surface. Other aerosols (like soot) directly absorb solar radiation, leading to local heating of the atmosphere, and some absorb and emit infrared radiation. A further influence of aerosols is that many act as nuclei on which cloud droplets condense, affecting the number and size of droplets in a cloud and hence altering the reflection and absorption of solar radiation by the cloud and the lifetime of the cloud (Stevens and Feingold, 2009). The precise nature of aerosol/cloud interactions and how they interact with the water cycle remains a major uncertainty in our understanding of climate processes. Because man-made aerosols are mostly introduced near the Earth's surface, they are washed out of the atmosphere by rain in typically a few days. They thus remain mostly concentrated near their sources and affect climate with a very strong regional pattern, usually producing cooling.

In contrast, GHGs such as CO_2 and CH_4 have lifetimes of decades or much longer. As a result, they are globally mixed and concentrations build up over time. GHG concentrations in the atmosphere have increased markedly as a result of human activities since 1750, and they are now higher than at any time in at least the last 650,000 years. It took at least 10,000 years from the end of the last ice age (18,000 years ago) for levels of CO_2 to increase 100 parts per million (ppm) by volume to 280 ppm, but that same increase has occurred over only the past 150 years to current values in excess of 385 ppm (Figure 2.1). About half of that increase has occurred over the last 35 years, owing mainly to combustion of fossil fuels and changes in land use. The CO_2 concentration growth rate was larger during the last decade than it has been since the beginning of continuous direct measurements in the late 1950s. In the absence of controls, future projections are that the rate of increase in CO_2 amount may accelerate, and concentrations could double from pre-industrial values within the next 50–100 years.

Methane is the second most important anthropogenic GHG. Predominantly because of agriculture and fossil fuel use, the global atmospheric concentration of CH_4 has increased from a pre-industrial

value of 715 part per billion (ppb) by volume to 1774 ppb in 2005, although growth rates have declined since the early 1990s, consistent with total emissions (natural and anthropogenic sources) being nearly constant over this period. Global N_2O concentrations have also increased significantly from pre-industrial values. Together, the combined radiative forcing from these three GHGs is +2.3 Watts per square metre (W/m^2), relative to 1750, which dominates the total net anthropogenic forcing (+1.6 W/m^2). The total net anthropogenic forcing includes contributions from aerosols (a negative forcing) and several other sources, such as tropospheric ozone and halocarbons.

Climate model simulations that account for such changes in forcings have now reliably shown that global surface warming of recent decades is a response to the increased concentrations of GHGs

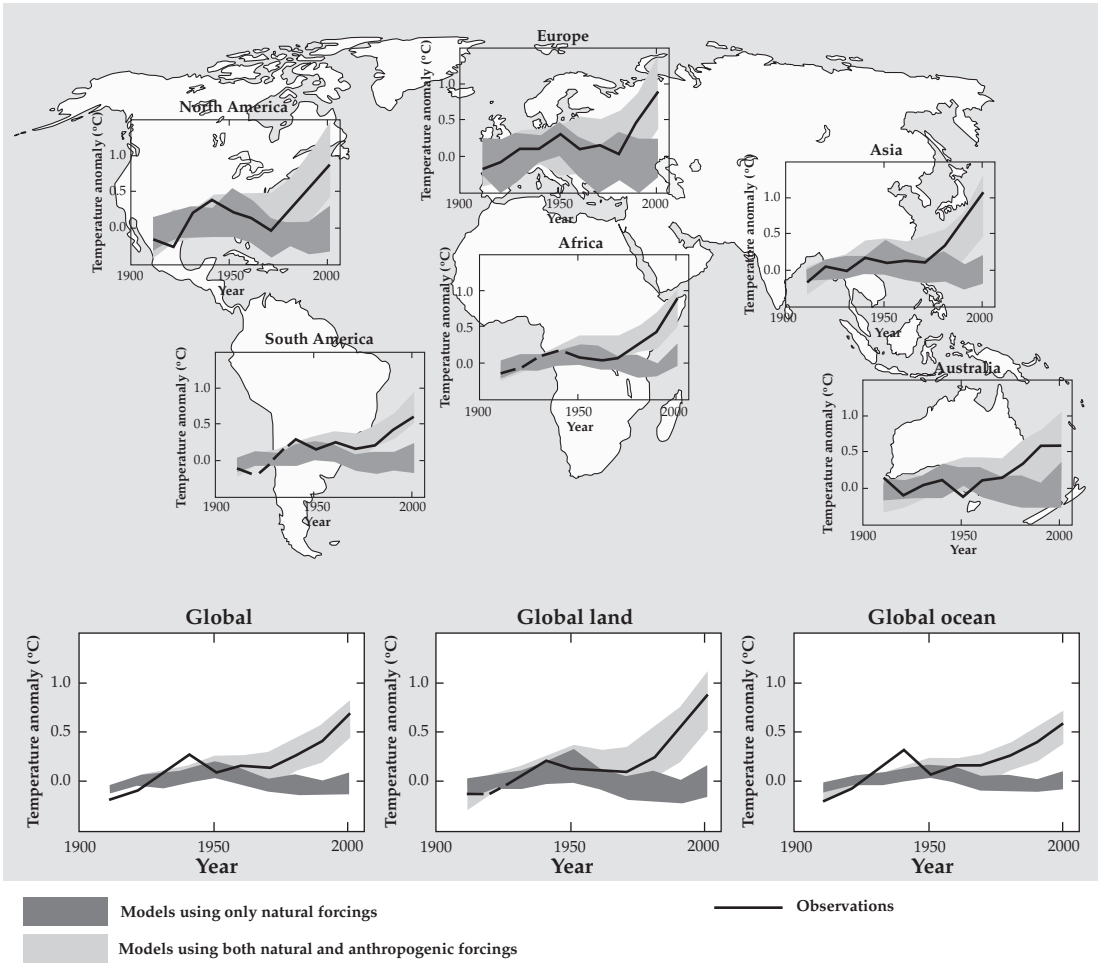

Figure 2.2 Comparison of observed continental- and global-scale changes in surface temperature with results simulated by climate models using natural and anthropogenic forcings. Decadal averages of observations are shown for 1906–2005 (black line) plotted against the centre of the decade and relative to the corresponding average for 1901–1950. Lines are dashed where spatial coverage is less than 50%. Dark shaded bands show the 5–95% range for 19 simulations from five climate models using only the natural forcings due to solar activity and volcanoes. Light shaded bands show the 5–95% range for 58 simulations from 14 climate models using both natural and anthropogenic forcings. The figure is taken from the Fourth Assessment Report of the Intergovernmental Panel on Climate Change Working Group I Summary for Policymakers (IPCC, 2007a). See Plate 1.

and sulphate aerosols in the atmosphere. When the models are run without these forcing changes, the remaining natural forcings and intrinsic natural variability fail to capture the almost linear increase in global surface temperatures over the past 40 years or so, but when the anthropogenic forcings are included, the models simulate the observed global temperature record with impressive fidelity (Figure 2.2). Changes in solar irradiance since 1750 are estimated to have caused a radiative forcing of +0.12 W/m^2, mainly in the first part of the 20th century. Prior to 1979, when direct observations of the sun from space began, changes in solar irradiance are more uncertain, but direct measurements show that the sun has not caused warming since 1979. Moreover, the models indicate that volcanic and anthropogenic aerosols have offset some of the additional warming that would have resulted from observed increases in GHG concentrations alone. For instance, since about 2000 the sunspot cycle went from a maximum to a minimum and a very quiet sun, decreasing total solar irradiance by 0.1%. This has contributed a slight cooling component to the planet, perhaps offsetting about 10–15% of the recent warming.

A significant advancement since the Third Assessment Report (TAR) of IPCC in 2001 is that a larger number of simulations available from a broader range of models allows for a more definitive evaluation of the role of various forcings in producing not only changes in global average temperature but also changes in continental and ocean basin-scale temperatures. The patterns of warming over each continent except Antarctica and each ocean basin over the past 50 years are only simulated by models that include anthropogenic forcing (Figure 2.2). Attribution studies have also demonstrated that many of the observed changes in indicators of climate extremes consistent with warming, including the annual number of frost days, warm and cold days, and warm and cold nights, have likely occurred as a result of increased anthropogenic forcing. In other words, many of the recently observed changes in climate are now being simulated in models.

The ability of coupled climate models to simulate the temperature evolution on continental scales, and the detection of anthropogenic effects on each continent except Antarctica, provides even stronger evidence of human influence on the global climate than was available to the TAR. No climate model that has used natural forcing only has reproduced either the observed global mean warming trend or the continental mean warming trends. Attribution of temperature change on smaller than continental scales and over time scales of less than 50 years or so is more difficult because of the much larger signal of natural variability on smaller space and time scales (Hawkins and Sutton, 2009).

2.3 Observed changes in surface climate

2.3.1 Temperature

The globe is warming dramatically compared with natural historical rates of change (IPCC, 2007a). Global surface temperatures today are more than 0.75°C warmer than at the beginning of the 20th century, and rates of temperature rise are greatest in recent decades (Figure 2.1). Over the last 50 years, the rate of warming is nearly double that of the 100-year trend, and 12 of the 14 warmest years in the global surface temperature record have occurred since 1995. The period since 2001 is ~0.2°C warmer than the 1991–2000 decade. Global land regions have warmed the most (0.7°C) since 1979, with the greatest warming in the boreal winter and spring months over the NH continents.

There is a very high degree of confidence in the global surface temperature values and the change estimates presented in Figure 2.1. The maximum difference, for instance, among three independent estimates of global surface temperature change since 1979 is 0.01°C/decade. Spatial coverage has improved, and daily temperature data for an increasing number of land stations have also become available, allowing more detailed assessments of extremes, as well as potential urban influences on both large-scale temperature averages and microclimate. It is well documented, for instance, that urban heat island effects are real, but very local, and they have been accounted for in the analyses: the urban heat island influence on continental, hemispheric, and global average trends is at least an order of magnitude smaller than decadal and longer time-scale trends, as cities make up less than 0.5% of global land areas (see Schneider *et al.*, 2009).

There is no urban heat bias in the SST record. Over the global oceans, surface temperatures have

warmed 0.35°C since 1979, and the warming is strongly evident at all latitudes over each of the ocean basins. Moreover, the warming is evident at depth as well, indicating that the ocean is absorbing most of the heat being added to the climate system. The largest short-term fluctuations in global mean temperatures come from El Niño and La Niña events. Heat stored in the ocean is released during an El Niño, and this contributes to increases in global temperatures. From late 2007 to the first part of 2009, lower temperatures occurred in association with the large 2007–2008 La Niña event, followed by a weaker La Niña in 2008–2009. The highest global mean SSTs recorded in the instrumental record occurred in the middle of 2009 as a substantial El Niño developed.

2.3.2 Sea level

The ocean warming causes sea water to expand and thus contributes to sea level rise. Melting of glaciers on land as well as ice caps and ice sheets also contributes. Instrumental measurements of sea level indicate that the global average has increased approximately 17 cm over the last century, and the increase has been 0.18 cm per year since 1961. The rate has been even faster recently (about 0.31 cm per year from 1993 thorough mid-2009), when truly global values have been measured from altimeters in space. Prior to 2004, about 60% of global sea level rise is from ocean warming and expansion, while 40% was from melting land ice adding to the ocean volume. Since 2004 melting ice sheets have contributed more. The observation of consistent global sea level rise over several decades, and also an increasing rate of sea level rise in the last decade or so, is probably the single best metric of the cumulative global warming experienced to date. A consequence is an increasing risk of coral bleaching and coastal storm surge flooding.

2.3.3 Snow cover, sea and land ice

The observed increases in surface temperature are consistent with nearly worldwide reductions in glacier and small ice cap mass and extent in the 20th century. In addition, flow speed has recently increased for some Greenland and Antarctic outlet glaciers, which drain ice from the interior, and melting of Greenland and West Antarctica has increased after about 2000. Critical changes (not well measured) are occurring in the ocean and ice shelves that buttress the flow of glaciers into the ocean. Glaciers and ice caps respond not only to temperature but also to changes in precipitation, and both winter accumulation and summer melting have increased over the last half century in association with temperature increases. In some regions, moderately increased accumulation observed in recent decades is consistent with changes in atmospheric circulation and associated increases in winter precipitation (e.g. southwestern Norway, parts of coastal Alaska, Patagonia, and the South Island of New Zealand) even though increased ablation has led to marked declines in mass balances in Alaska and Patagonia. Tropical glacier changes are synchronous with those at higher latitudes, and all have shown declines in recent decades. Decreases in glaciers and ice caps contributed to sea level rise by 0.05 cm per year from 1961 to 2003, and 0.08 cm per year from 1993 to 2003. Taken together, shrinkage of the ice sheets of Greenland and Antarctica contributed 0.04 cm per year to sea level rise over 1993–2003. Since then evidence suggests increased melting of both Greenland and Antarctica, whereby they contribute (about equally) about 0.1 cm per year to sea level rise.

Snow cover has decreased in many NH regions, particularly in the spring season, and this is consistent with greater increases in spring than autumn surface temperatures in middle latitude regions. Sea ice extents have decreased in the Arctic, particularly in the spring and summer seasons (7.4%/decade decrease from 1978 to 2005), and this is consistent with the fact that the average annual Arctic temperature has increased at almost twice the global average rate, although changes in winds are also a major factor. The AR4 included data only to 2005, when sea ice extents were at record low values, which was also the warmest year since records began in 1850 for the Arctic north of 65°N. This record was smashed in 2007 when Arctic sea ice dropped to over 20% below the 2005 value. There have also been decreases in sea ice thickness. With an unprecedented amount of first year ice in the Arctic that is very vulnerable to melting, 2008 ranks slightly higher in terms of sea ice extent than 2007, and 2009

ranks third, but still lower than 2005. The total peak summer time decrease in Arctic sea ice is about 40% of the 1970s' values. Temperatures at the top of the permafrost layer in the Arctic have increased since the 1980s (up to 3°C locally), and the maximum area covered by seasonally frozen ground has decreased by about 7% in the NH since 1900, with an even greater decrease (15%) in the boreal spring. There has been a reduction of about 2 weeks in the annual duration of northern lake and river ice cover.

In contrast to the Arctic, Antarctic sea ice did not exhibit any significant trend from the end of the 1970s through to 2006, which is consistent with the lack of trend in surface temperature south of 65°S over that period. However, along the Antarctic Peninsula where significant warming has been observed, progressive break up of ice shelves occurred beginning in the late 1980s, culminating in the break up of the Larsen-B ice shelf in 2002. Antarctic conditions are uniquely influenced by the ozone hole, which alters the atmospheric circulation over the southern regions.

2.3.4 Extremes

For changes in mean temperature, there is likely to be an amplified change in extremes. Extreme events, such as heat waves, are exceedingly important to both natural systems and human systems and infrastructure. People and ecosystems are adapted to a range of natural weather variations, but it is the extremes of weather and climate that exceed tolerances. Widespread changes in temperature extremes have been observed over the last 50 years. In particular, the number of heat waves globally has increased, and there have been widespread increases in the numbers of warm nights. Cold days, cold nights, and days with frost have become rarer. Such changes greatly affect the range of animals, including birds.

Satellite records suggest a global trend towards more intense and longer-lasting tropical cyclones (including hurricanes and typhoons) since about 1970, correlated with observed warming of tropical SSTs. There is no clear trend in the annual number of tropical cyclones globally, although a substantial increase has occurred in the North Atlantic after 1994. There are concerns about the quality of tropical cyclone data, particularly before the satellite era. Furthermore, strong multi-decadal variability is observed and complicates detection of long-term trends in tropical cyclone activity. It has been estimated that heavy rains in tropical storms and hurricanes have increased by 6–8% as a result of higher SSTs and more water vapour in the atmosphere (Trenberth, 2007).

2.3.5 Precipitation and drought

Changes are also occurring in the amount, intensity, frequency, and type of precipitation in ways that are also consistent with a warming planet. These aspects of precipitation generally exhibit large natural variability compared to temperature, making it harder to detect trends in the observational record. A key ingredient in changes in character of precipitation is the observed increase in water vapour and thus the supply of atmospheric moisture to all storms, increasing the intensity of precipitation events. Widespread increases in heavy precipitation events and risk of flooding have been observed, even in places where total amounts have decreased. Hence, the frequency of heavy rain events has increased in most places but so too has episodic heavy snowfall events that are thus associated with warming.

Long-term (1900–2005) trends have been observed in total precipitation amounts over many large regions. Significantly increased precipitation has been observed in eastern parts of North and South America, northern Europe, and northern and central Asia. Drying has been observed in the Sahel, the Mediterranean, southern Africa, and parts of southern Asia. Precipitation is highly variable spatially and temporally. Robust long-term trends have not been observed for other large regions. The pattern of precipitation change is one of increases generally at higher northern latitudes (because as the atmosphere warms it holds more moisture) and drying in the tropics and subtropics over land. Basin-scale changes in ocean salinity provide further evidence of changes in the Earth's water cycle, with freshening at high latitudes and increased salinity in the subtropics.

More intense and longer droughts have been observed over wider areas since the 1970s, particularly in the tropics and subtropics. Increased drying due to higher temperatures and decreased precipitation have contributed to these changes, with the latter

being the dominant factor. The regions where droughts have occurred are determined largely by changes in SST, especially in the tropics (such as during El Niño), through changes in the atmospheric circulation and precipitation. In the western USA, diminishing snow pack and subsequent summer soil moisture reductions have also been a factor. In Australia and Europe, direct links to warming have been inferred through the extreme nature of high temperatures and heat waves accompanying drought.

In summary, there are an increasing number of many independent surface observations that give a consistent picture of a warming world. Such multiple lines of evidence, the physical consistency among them, and the consistency of findings among multiple, independent analyses form the basis for the iconic phrase from IPCC (2007a) that the 'warming of the climate system is unequivocal'.

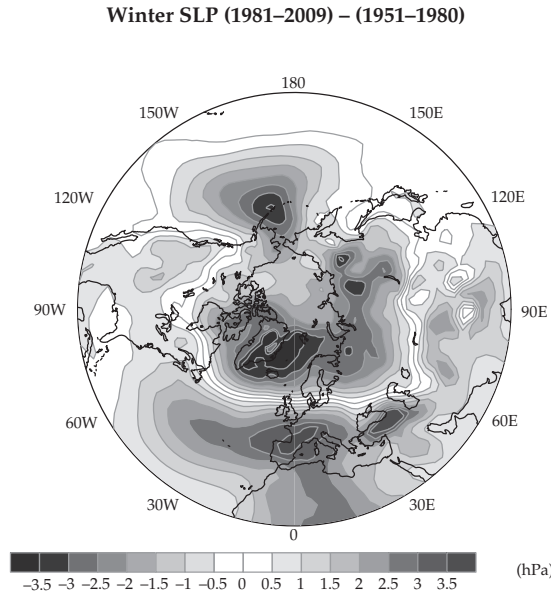

Figure 2.3 Boreal winter (December–March) average Northern Hemisphere sea level pressure (SLP) anomalies (hPa) since 1981 expressed as departures from the 1951–1980 average values. The SLP data are from Trenberth and Paolino (1980). See Plate 2.

2.4 Observed changes in atmospheric circulation

2.4.1 Sea level pressure

Much of the warming that has contributed to the global temperature increases of recent decades (Figure 2.1) has occurred during boreal winter and spring over the continents of the NH. This pattern of warming is strongly related to decade-long changes in natural patterns of the atmospheric and oceanic circulation. The changes in boreal winter circulation are reflected by lower-than-average sea level pressure (SLP) over the middle and high latitudes of the North Pacific and North Atlantic Oceans, as well as over much of the Arctic, and higher-than-average SLP over the subtropical Atlantic (Figure 2.3).

Over the North Pacific, the changes in SLP correspond to an intensification of the Aleutian low-pressure system, while over the North Atlantic the changes correspond to intensified low- and high-pressure centres near Iceland and the Azores, respectively. These northern oceanic pressure systems are semi-permanent features of the winter atmospheric circulation (e.g. Hurrell and Deser, 2009). Over the SH, similar changes have been observed during austral summer, with surface pressures lowering over the Antarctic and rising over middle latitudes since the late 1970s. The long-term significance of the SH SLP change is more difficult to establish, however, given the greater paucity of historical data over the southern ocean and Antarctica.

2.4.2 Winds and storm tracks

Because air flows counterclockwise around low pressure and clockwise around high pressure in the NH, westerly flow across the middle latitudes of the Atlantic and Pacific sectors occurs throughout the year. The vigour of the flow is related to the north–south (meridional) pressure gradient, so the surface winds are strongest during winter when they average more than 5 m/s from the eastern USA across the Atlantic onto northern Europe as well as across the entire Pacific. These middle latitude westerly winds extend throughout the troposphere and reach their maximum (up to more than 40 m/s in the mean) at a height of about 12 km. This 'jet stream' roughly coincides with the path of storms travelling across the northern oceans onto the continents. These storm tracks play a critical role in both weather

and climate, as they are associated with much of the precipitation and severe weather in middle latitudes and they transport large amounts of heat, moisture, and momentum towards the poles.

Several studies, assessed by IPCC (2007a), indicate that there has been a poleward shift in the mean latitude of extratropical cyclones, and that cyclones have become fewer and more intense, over the last half of the 20th century. For instance, the change towards a deeper polar vortex and Icelandic Low in boreal winter (Figure 2.3) has been accompanied by intensification and poleward displacement of the Atlantic jet and associated enhancement of the Atlantic storm track activity. Analogous changes have also been found over the North Pacific and in the SH.

There are, however, significant uncertainties, with some studies suggesting that storm track activity during the last part of the 20th century may not be more intense than the activity prior to the 1950s. Station pressure data over the Atlantic–European sector (where records are long and consistent) show a decline of storminess from high levels during the late 19th century to a minimum around 1960 and then a quite rapid increase to a maximum around 1990, followed again by a slight decline. Changes in storm tracks, however, are complex and are related to spatial shifts and strength changes in leading patterns of climate variability (next section).

2.5 Observed changes in patterns of circulation variability

2.5.1 Teleconnections

A consequence of the transient behaviour of atmospheric planetary-scale waves is that anomalies in climate on seasonal time scales typically occur over large geographic regions. Some regions may be cooler than average, while at the same time, thousands of kilometres away, warmer conditions prevail. These simultaneous variations in climate, often of opposite sign, over distant parts of the globe are commonly referred to as 'teleconnections' in the meteorological literature. Though their precise nature and shape vary to some extent according to the statistical methodology and the data set employed in the analysis, consistent regional characteristics that identify the most conspicuous patterns emerge. Understanding the nature of teleconnections and changes in their behaviour is central to understanding regional climate variability and change, as well as impacts on humans and ecosystems.

The analysis of teleconnections has typically employed a linear perspective, which assumes a basic spatial pattern with varying amplitude and mirror image positive and negative polarities. In contrast, non-linear interpretations identify preferred climate anomalies as recurrent states of a specific polarity. Climate change may result through changes from one quasi-stationary state to another, as a preference for one polarity of a pattern, or through a change in the nature or number of states.

Arguably the most prominent teleconnections over the NH are the North Atlantic Oscillation (NAO) and the Pacific–North American (PNA) patterns, and their spatial structures are revealed most simply through one-point correlation maps (Figure 2.4). In the SH, wave structures do not emerge as readily owing to the dominance of more zonally symmetric variability (the so-called southern annular mode, or SAM, see Section 2.5.6). Although teleconnections are best defined over a grid, simple indices based on a few key station locations remain attractive, as the series can often be carried back in time long before complete gridded fields were available. The disadvantage of such station-based indices is increased noise from the reduced spatial sampling. For instance, Hurrell *et al.* (2003) found that the residence time of the NAO in its positive phase in the early 20th century was not as great as indicated by the positive NAO index for that period.

Many teleconnections have been identified, but combinations of only a small number of patterns can account for much of the interannual variability in the circulation and surface climate. Quadrelli and Wallace (2004) found that many patterns of NH interannual variability can be reconstructed as linear combinations of the first two empirical orthogonal functions (EOFs) of SLP. Trenberth *et al.* (2005) analysed global atmospheric mass and found four key rotated EOF patterns: the two annular modes (SAM and the northern annular mode, or NAM), a global ENSO-related pattern, and a fourth closely

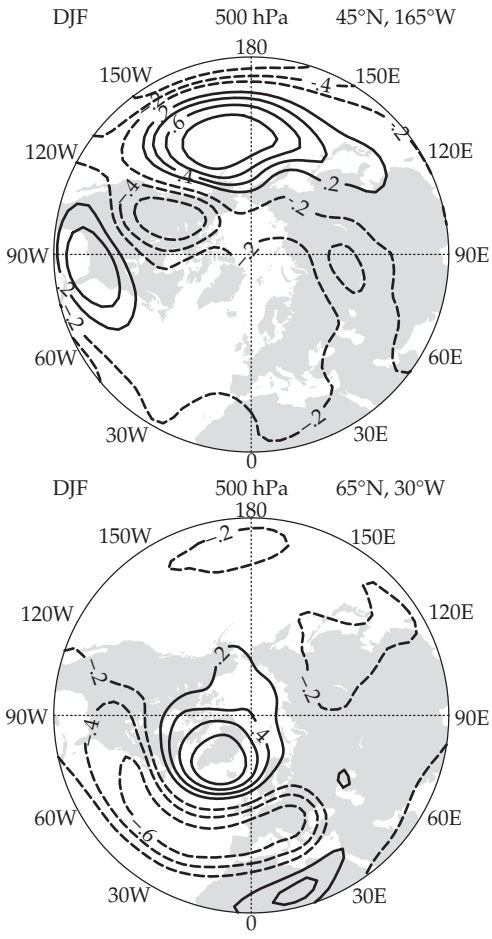

Figure 2.4 One-point correlation maps of 500 hPa geopotential heights for boreal winter (December–February, DJF) over 1958–2006. In the top panel, the reference point is 45°N, 165°W, corresponding to the primary centre of action of the Pacific–North American pattern. In the lower panel, the North Atlantic Oscillation pattern is illustrated based on a reference point of 65°N, 30°W. Negative correlation coefficients are dashed, the contour increment is 0.2 and the zero contour has been excluded. Adapted from Hurrell and Deser (2009).

related to the North Pacific index (NPI) and the Pacific decadal oscillation (PDO), which in turn is closely related to ENSO and the PNA pattern.

Teleconnection patterns tend to be most prominent in winter (especially in the NH), when the mean circulation is strongest. The strength of teleconnections and the way they influence surface climate also vary over long time scales, and these aspects are exceedingly important for understanding regional climate change. In the following only the predominant teleconnection patterns are documented.

2.5.2 ENSO

Fluctuations in tropical Pacific SSTs are related to the occurrence of El Niño, during which the equatorial surface waters warm considerably from the International Date Line (IDL) to the west coast of South America. The atmospheric phenomenon tied to El Niño is termed the Southern Oscillation, which is a global-scale standing wave in atmospheric mass (thus evident in SLP), involving exchanges of air between Eastern and Western Hemispheres centred in tropical and subtropical latitudes (Figure 2.5). The oscillation is characterized by the inverse variations in SLP at Darwin (12.4°S, 130.9°E) in northern Australia and Tahiti (17.5°S, 149.6°W) in the south Pacific: annual mean pressures at these two stations are correlated at –0.8. A simple index of the SO is, therefore, often defined by the Tahiti minus Darwin SLP anomalies, normalized by the long-term mean and standard deviation of the mean SLP difference, or simply by the negative of the Darwin record (Figure 2.5 and Table 2.1). During an El Niño event, the SLP tends to be higher than usual at Darwin and lower than usual at Tahiti. Negative values of the SO index (SOI), therefore, are typically associated with warmer-than-average SSTs in the near equatorial Pacific, while positive values of the index are typically associated with colder-than-average SSTs. While changes in near equatorial Pacific SSTs can occur without a swing in the SO, El Niño (EN) and the SO are linked so closely that the term ENSO is used to describe the atmosphere–ocean interactions over the tropical Pacific. Warm ENSO events, therefore, are those in which both a negative SO extreme and an El Niño occur together.

During the warm phase of ENSO, the warming of the waters in the central and eastern tropical Pacific shifts the location of the heaviest tropical rainfall eastward towards or beyond the IDL from its climatological position centred over Indonesia and the far western Pacific. This shift in rainfall alters the heating patterns that force large-scale waves in the atmosphere. The waves in the airflow determine the preferred location of the extratropical storm tracks. Consequently, changes from one phase of the SO to

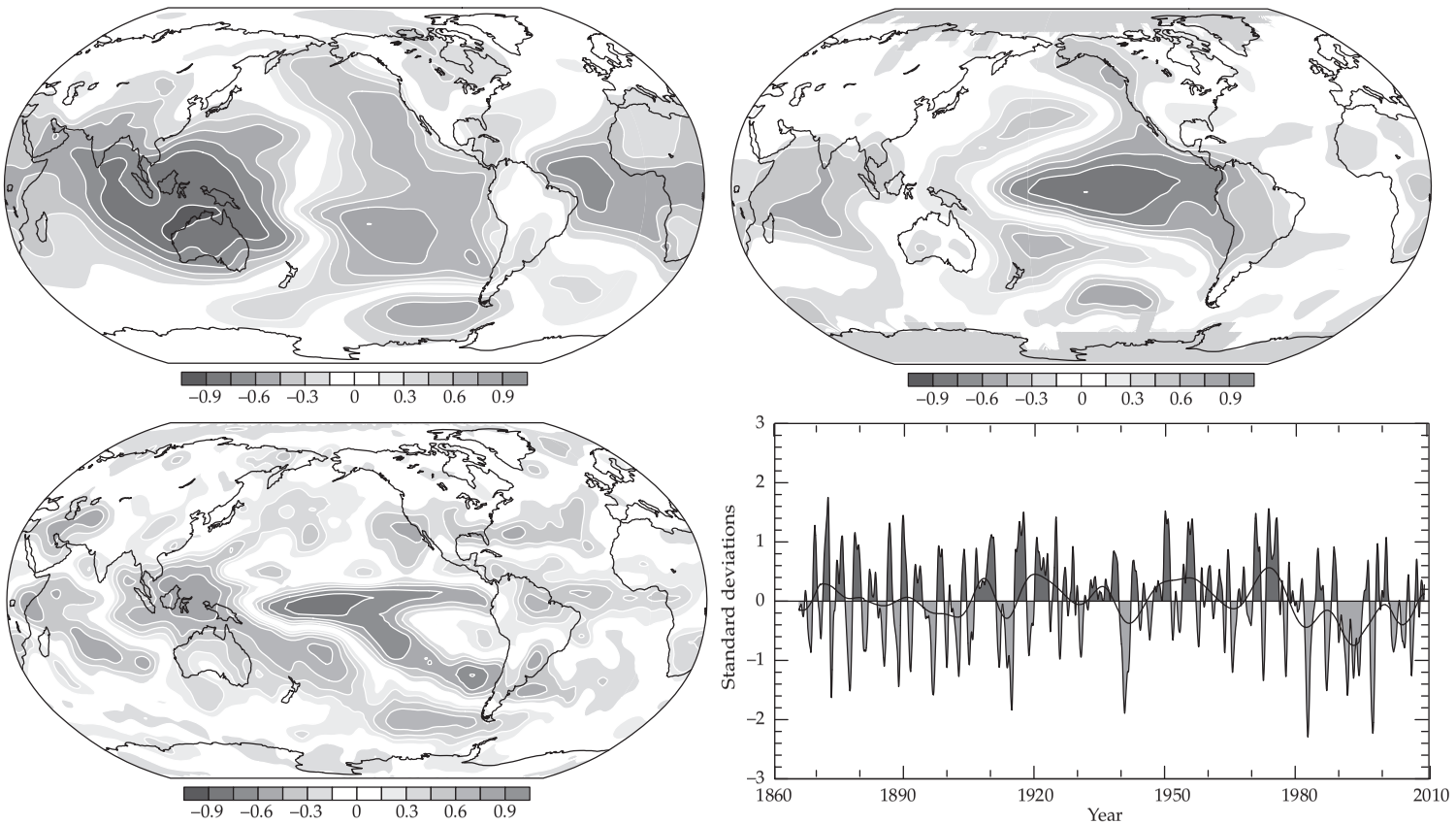

Figure 2.5 Correlations with the Southern Oscillation index (SOI) (Table 2.1) for annual (May–April) means for sea level pressures (SLP; top left) and surface temperature (top right) for 1958–2004, and estimates of global precipitation for 1979–2003 (bottom left), updated from Trenberth and Caron (2000) and IPCC (2007a). The Darwin-based SOI, in normalized units of standard deviation, from 1866 to 2009 (lower right) features monthly values with an 11-point low-pass filter, which effectively removes fluctuations with periods of less than 8 months. The smooth black curve shows decadal variations. Red values indicate positive SLP anomalies at Darwin and thus El Niño conditions. See Plate 3.

another have a profound impact on regional temperatures (Figure 2.5). Most warm phase ENSO winters, for example, are mild over western Canada and parts of the northern USA and are cool over the southern USA, although the regional details vary considerably from one event to another.

Although the SO has a typical period of 2–7 years, the strength of the oscillation has varied considerably over the instrumental period of record. There were strong variations from the 1880s to the 1920s and after about 1950, but weaker variations in between (with the exception of the major 1939–1941 event). A remarkable feature of the SOI is the decadal and longer-term variations in recent years, which is lacking from earlier periods. In particular, a pronounced change towards more negative values, and thus warmer tropical Pacific conditions, is evident since the mid-1970s, including a shift to generally above-normal SSTs in the eastern and central equatorial Pacific and a tendency towards more prolonged and stronger El Niño events.

ENSO events involve large exchanges of heat between the ocean and atmosphere and affect global mean temperatures. The 1997–1998 event was the largest on record in terms of SST anomalies, and the global mean temperature in 1998 was the highest on record. Extremes of the hydrological cycle such as floods and droughts are common with ENSO and are apt to be enhanced with global warming. For example, the modest 2002–2003 El Niño was associated with a drought in Australia, made much worse by record-breaking heat. A strong La Niña event took place in 2007–2008, contributing to 2008 being the coolest year since the turn of the 21st century, and was followed by a weak La Niña in 2008–2009. However, the transition to El Niño by June 2009 has led to the highest global SST anomaly in July 2009, exceeding the previous record in 1998. Thus, whether or not observed changes in ENSO behaviour are physically linked to global climate change is a research question of great importance.

2.5.3 Extratropical Pacific

In the middle troposphere, the warm phase ENSO pattern is typically associated with higher-than-normal pressure near Hawaii and over the northwestern USA and western Canada, while pressures are typically lower than normal over the central North Pacific and the southeast USA, i.e. a positive PNA teleconnection pattern (Figure 2.4). The difference in normalized height anomalies from these four centres forms the most commonly used time-varying index of the PNA (Table 2.1). Variations in the PNA pattern represent changes in the north–south migration of the large-scale PNA air masses,

Table 2.1 Indices of circulation variability.

Southern Oscillation Index (SOI). The Tahiti minus Darwin SLP anomalies, normalized by the long-term mean and standard deviation of the mean SLP difference, or alternatively by the negative of the Darwin SLP record (www.cgd.ucar.edu/cas/catalog/climind/soi.html)

Pacific—North American pattern (PNA) Index. The mean of normalized 500 hPa height anomalies at 20°N, 160°W and 55°N,115°W minus those at 45°N, 165°W and 30°N, 85°W (www.cpc.noaa.gov/products/precip/CWlink/pna/month_pna_index2.shtml)

North Pacific Index (NPI). The average SLP anomaly over the Gulf of Alaska (30°N–65°N, 160°E–140°W; www.cgd.ucar.edu/cas/jhurrell/indices.html)

Pacific Decadal Oscillation (PDO) Index. The amplitude of the pattern defined by the leading EOF of annual mean SST in the Pacific basin north of 20°N (http://jisao.washington.edu/pdo/PDO.latest)

Atlantic Multi-decadal Oscillation (AMO) Index. The low-pass filtered time series of annual mean SST anomalies averaged over the North Atlantic (0–60°N, 0–80°W; www.cgd.ucar.edu/cas/catalog/climind/AMO.html)

North Atlantic Oscillation (NAO) Index. The difference of normalized winter (December–March) SLP anomalies between Lisbon, Portugal and Stykkisholmur, Iceland, or alternatively the amplitude of the leading EOF of mean SLP over the North Atlantic (20–80°N, 90°W–40°E; www.cgd.ucar.edu/cas/jhurrell/indices.html)

Northern Annular Mode (NAM) Index. The amplitude of the pattern defined by the leading EOF of winter monthly mean NH SLP anomalies poleward of 20°N (www.cgd.ucar.edu/cas/jhurrell/indices.html)

Southern Annular Mode (SAM) Index. The difference in average SLP between SH middle and high latitudes (usually 45°S and 65°S) from gridded or station data (www.antarctica.ac.uk/met/gjma/sam.html), or alternatively the amplitude of the leading EOF of monthly mean SH 850 hPa height poleward of 20°S

storm tracks and their associated weather, affecting precipitation in western North America and the frequency of Alaskan blocking events and associated cold air outbreaks over the western USA in winter. On interannual time scales, the association between PNA and ENSO variations reflects mainly the dynamical teleconnection to higher latitudes forced by deep convection in the tropics.

At the surface, the signature of the PNA is mostly confined to the North Pacific, where SLP tends to be lower than normal during ENSO. Moreover, decadal to inter-decadal variability in the atmospheric circulation is especially prominent in the North Pacific (e.g. Trenberth and Hurrell, 1994) where fluctuations in the strength of the wintertime Aleutian low-pressure system, indicated by the NPI (Table 2.1), covary with North Pacific SST in what has been termed the 'Pacific Decadal Oscillation' or PDO. The NPI (Figure 2.6) reveals extended periods of predominantly high values indicative of a weakened circulation (1900–1924 and 1947–1976) and predominantly low values indicative of strengthened circulation (1925–1946 and 1977–2005). The well-known decrease in pressure from 1976 to 1977 is analogous to transitions that occurred from 1946 to 1947 and from 1924 to 1925, and these earlier changes were also associated with SST fluctuations in the tropical Indian and Pacific Oceans (e.g. Deser *et al.*, 2004).

Very similar time-scale fluctuations in SST and atmospheric and ocean circulations are present across the whole Pacific basin, and these variations are known as the inter-decadal Pacific oscillation (IPO). The PDO/IPO has been described as a long-lived El Niño-like pattern of Indo-Pacific climate variability or as a low-frequency residual of ENSO variability on multi-decadal time scales. Phase changes of the PDO/IPO are associated with pronounced changes in temperature and rainfall patterns across North and South America, Asia and Australia. Furthermore, ENSO teleconnections on interannual time scales around the Pacific basin are significantly modified by the PDO/IPO.

2.5.4 Atlantic multi-decadal oscillation

Over the Atlantic sector, in contrast to the tropical Pacific, decadal variability has large amplitude relative to interannual variability, especially over the North Atlantic (e.g. Knight *et al.*, 2005). The Atlantic decadal variability has been termed the 'Atlantic multi-decadal oscillation' or AMO (Figure 2.7; Table 2.1). North Atlantic SSTs show a 65–75-year

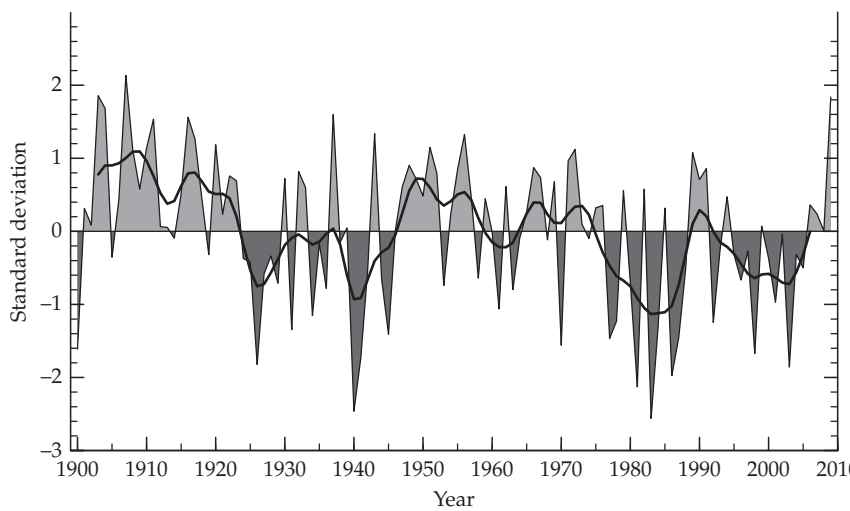

Figure 2.6 Time series of the North Pacific index (Table 2.1) reflecting the strength of the winter Aleutian low-pressure system, with positive (negative) values indicative of a weak (strong) Aleutian Low. The smooth black curve shows decadal variations. Values were updated and extended to earlier decades from Trenberth and Hurrell (1994).

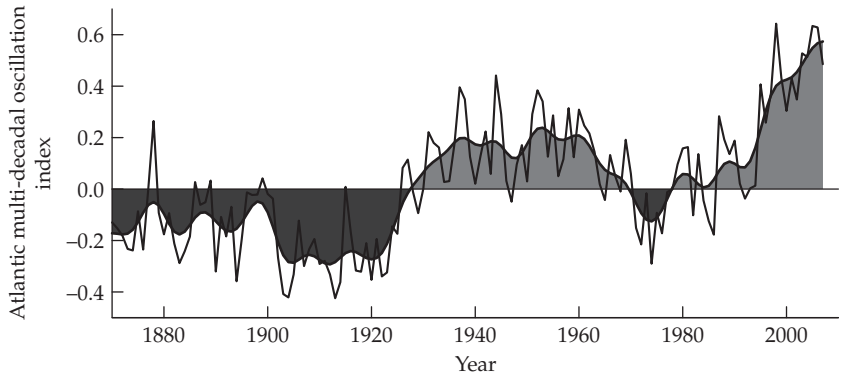

Figure 2.7 Atlantic multi-decadal oscillation as defined in Table 2.1. Updated from Trenberth and Shea (2006).

variation (0.4°C range), with a warm phase during 1930–1960 and cool phases during 1905–1925 and 1970–1990. The cycle appears to have returned to a warm phase beginning in the mid-1990s, and tropical Atlantic SSTs were at record high levels in 2005. Trenberth and Shea (2006) formed a revised AMO index, subtracting the global mean SST from the North Atlantic SST. The revised index is about 0.35°C lower than that in Figure 2.7 after 2000, highlighting the fact that most of the recent warming is global in scale. Instrumental records are not long enough to determine whether AMO variability has a well-defined period rather than a simpler character, such as 'red noise'. The robustness of the signal has therefore been addressed using paleoclimate records, and similar fluctuations have been documented through the last four centuries (e.g. Delworth and Mann, 2000).

The slow changes in Atlantic SSTs have affected regional climate trends over parts of North America and Europe, hemispheric temperature anomalies, sea ice concentration in the Greenland Sea, and hurricane activity in the tropical Atlantic and Caribbean (e.g. Webster *et al.*, 2005; Trenberth and Shea, 2006). In addition, tropical Atlantic SST anomalies have contributed to rainfall anomalies over the Caribbean and the Nordeste region of Brazil, and severe multi-year droughts over parts of Africa, including the Sahel (e.g. Hoerling *et al.*, 2006). Tropical Atlantic SST variations are also a factor in producing drought conditions over portions of North America, although tropical Pacific SST variations appear to play a more dominant role (e.g. Seager *et al.*, 2008).

2.5.5 North Atlantic Oscillation

One of the most prominent teleconnection patterns is the NAO, which refers to changes in the atmospheric SLP difference between the Arctic and the subtropical Atlantic (Figures 2.4 and 2.8). Although it is the only teleconnection pattern evident throughout the year in the NH, the climate anomalies associated with the NAO are largest during the boreal winter months, when the atmosphere is dynamically the most active.

A time series of nearly 150 years of wintertime NAO variability, the spatial pattern of the oscillation, and NAO impacts on winter surface temperature and precipitation are shown in Figure 2.8. Most modern NAO indices are derived either from the simple difference in surface pressure anomalies between various northern and southern locations or from the principal component time series of the leading (usually regional) EOF of SLP (Hurrell and Deser, 2009). A commonly used index (Figure 2.8; Table 2.1) is based on the differences in normalized SLP anomalies between Lisbon, Portugal, and Stykkisholmur, Iceland. This NAO index correlates with the NAM index (Table 2.1) at 0.85, which emphasizes that the NAO and NAM reflect essentially the same mode of tropospheric variability.

As reviewed in detail by Hurrell *et al.* (2003), the NAO exerts a dominant influence on winter surface temperatures across much of the NH, and on storminess and precipitation over Europe and North Africa (Figure 2.8). When the NAO index is

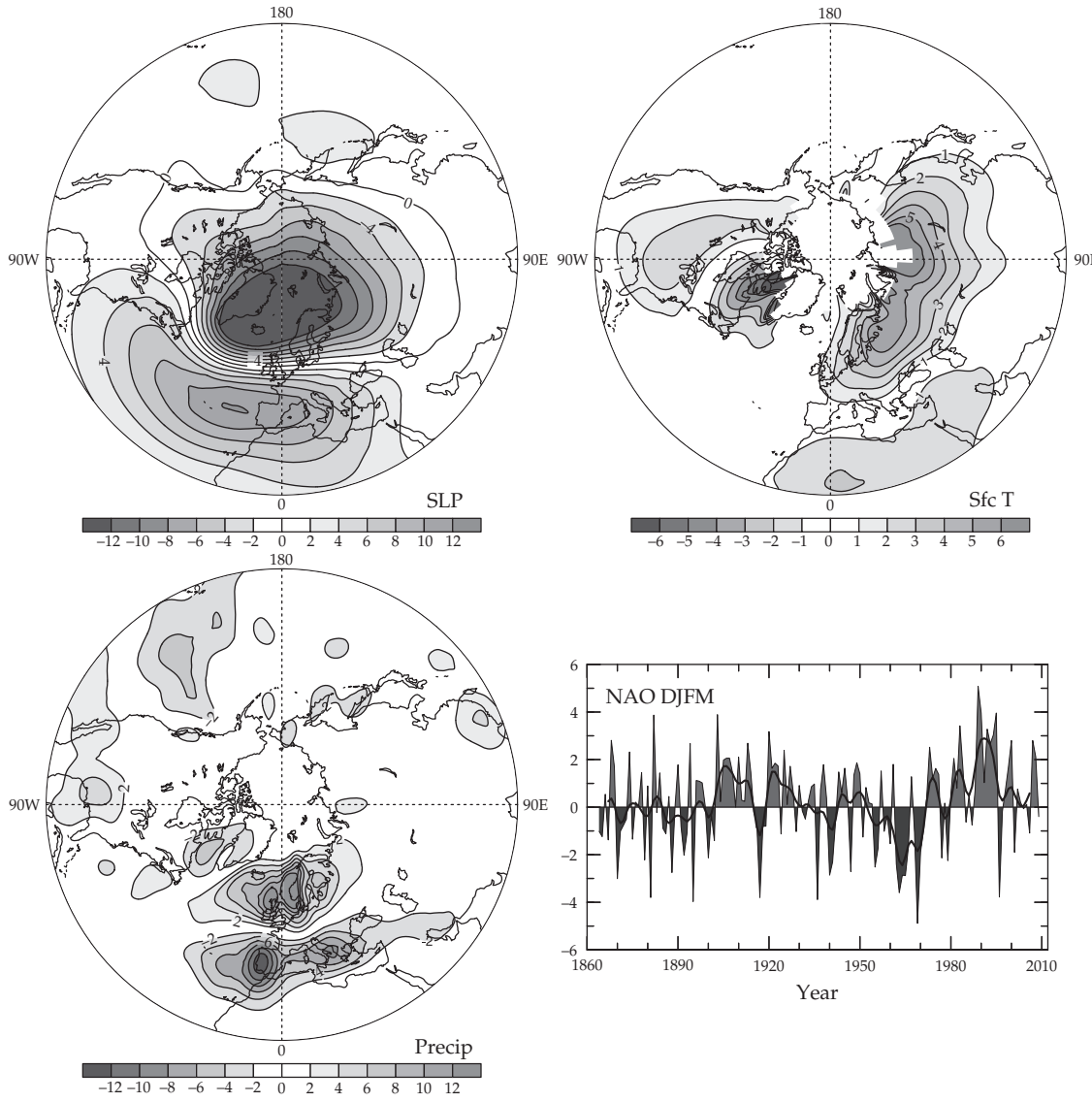

Figure 2.8 Changes in winter (December–March) surface pressure, temperature and precipitation corresponding to a unit deviation of the North Atlantic Oscillation (NAO) index over 1900–2009. Top left: Mean sea level pressure (0.1 hPa). Top right: Land surface air and SST (0.1°C; contour increment 0.2°C): regions of insufficient data (e.g. over much of the Arctic) are not contoured. Bottom left: Precipitation for 1979–2009 based on global estimates (0.1 mm/day; contour interval 0.6 mm/day). Bottom right: Station-based index of winter NAO (Table 2.1). The heavy solid line represents the index smoothed to remove fluctuations with periods less than 4 years. The indicated year corresponds to the January of the winter season (e.g. 1990 is the winter of 1989/1990). Adapted and updated from Hurrell *et al.* (2003) and IPCC (2007a). SLP, sea level pressure; Sfc T, surface temperature; Precip, precipitation; NAO, North Atlantic Oscillation;DJFM, December, January, February, March. See Plate 4.

positive, enhanced westerly flow across the North Atlantic in winter moves warm moist maritime air over much of Europe and far downstream, while stronger northerly winds over Greenland and northeastern Canada carry cold air southward and decrease land temperatures and SST over the northwest Atlantic. Temperature variations over North Africa and the Middle East (cooling) and the southeastern USA (warming), associated with the stronger clockwise flow around the subtropical Atlantic high-pressure centre, are also notable.

Positive NAO index winters are also associated with a northeastward shift in the Atlantic storm activity, with enhanced activity from Newfoundland into northern Europe and a modest decrease to the south. Positive NAO index winters are also typified by more intense and frequent storms in the vicinity of Iceland and the Norwegian Sea. The correlation between the NAO index and cyclone activity is highly negative in eastern Canada and positive in western Canada. The upward trend towards more positive NAO index winters from the mid-1960s to the mid-1990s was associated with increased wave heights over the northeast Atlantic and decreased wave heights south of 40°N.

The NAO modulates the transport and convergence of atmospheric moisture and the distribution of precipitation. More precipitation than normal falls from Iceland through Scandinavia during high NAO index winters, while the reverse occurs over much of central and southern Europe, the Mediterranean, parts of the Middle East, the Canadian Arctic, and much of Greenland (Figure 2.8). As far eastward as Turkey, river runoff is significantly correlated with NAO variability. There are also significant NAO effects on ocean heat content, sea ice, ocean currents, and ocean heat transport, as well as very significant impacts on many aspects of the north Atlantic/European biosphere (e.g. IPCC, 2007b). A thorough review of the response of terrestrial ecosystems to climate variability associated with the NAO is also provided by Mysterud *et al.* (2003), while Durant *et al.* (2004) review the impact of the NAO on North Atlantic marine birds (see also Kanuscak *et al.*, 2004).

2.5.6 Southern annular mode

The principal mode of variability of the atmospheric circulation in the SH is known as the SAM. It is essentially a zonally symmetric structure associated with synchronous pressure or height anomalies of opposite sign in middle and high latitudes, and therefore reflects changes in the main belt of subpolar westerly winds. Enhanced southern ocean westerlies occur in the positive phase of the SAM. The SAM contributes a significant proportion of SH mid-latitude circulation variability on many time scales. Trenberth *et al.* (2005) showed that the SAM is the leading mode in an EOF analysis of monthly mean global atmospheric mass, accounting for around 10% of total global variance.

As with the NAO/NAM, the structure and variability of the SAM result mainly from the internal dynamics of the atmosphere, and the SAM is an expression of storm track and jet stream variability. The SAM index (Figure 2.9; Table 2.1) reveals a general increase beginning in the 1960s consistent with a strengthening of the circumpolar vortex and intensification of the circumpolar westerlies. The trend in the SAM has contributed to Antarctic temperature trends, specifically a strong summer warming in the Peninsula region and little change or cooling over much of the rest of the continent.

The positive SAM is also associated with low pressure west of the Peninsula, leading to increased poleward flow, warming, and reduced sea ice in the region. The positive trend in the SAM has led to more cyclones in the circumpolar trough and hence a greater contribution to Antarctic precipitation from these near-coastal systems. The SAM also affects spatial patterns of precipitation variability in Antarctica and southern South America. Further aspects of the SAM, including its impacts, are summarized in IPCC (2007a).

2.6 Projected future climate change

The ability of climate models to simulate the past climate record gives us increased confidence in their ability to simulate the future. We can now look back at projections from earlier IPCC assessments and see that the observed rate of global warming since 1990 (about 0.2°C/decade) is

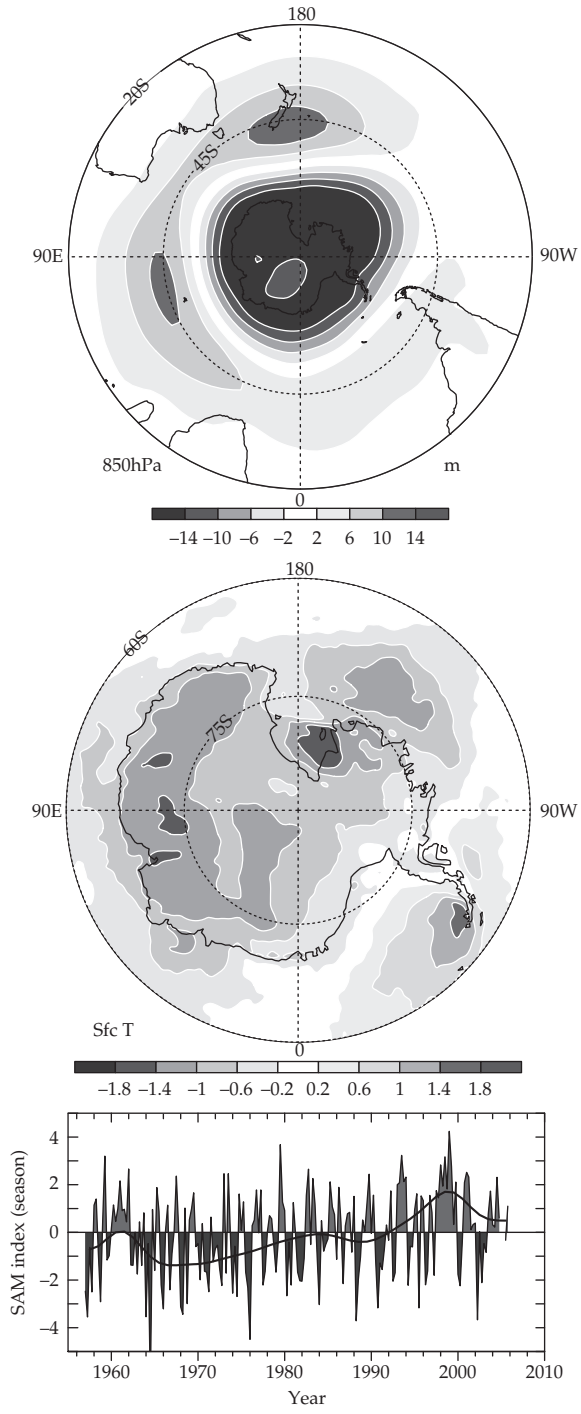

Figure 2.9 Bottom: Seasonal values of the southern annular mode (SAM) index (Table 2.1; updated from Marshall, 2003). The smooth black curve shows decadal variations. Top: The SAM geopotential height pattern as a regression based on the SAM time series for seasonal anomalies at 850 hPa (see also Thompson and Wallace, 2000). Middle: The regression of changes in surface temperature (°C) over the 23-year period (1982–2004) corresponding to a unit change in the SAM index, plotted south of 60°S. Values exceeding about 0.4°C in magnitude are significant at the 1% significance level. Adapted from IPCC (2007a). Sfc T, surface temperature. See Plate 5.

within the projected range (0.15–0.30°C/decade). Moreover, the attribution of the recent climate change to increased concentrations of GHGs in the atmosphere has direct implications for the future. Because of the long lifetime of CO_2 and the slow equilibration of the oceans, there is a substantial future commitment to further global climate change even in the absence of further emission of GHGs into the atmosphere. Several of the coupled model experiments performed for the IPCC AR4 explored the concept of climate change commitment. For instance, if concentrations of GHGs were held constant at year 2000 levels (implying a very large reduction in emissions), a further warming trend would occur over the next 20 years at a rate of about 0.1°C/decade, with a smaller warming rate continuing after that. Such committed climate change is due to (1) the long lifetime of CO_2 and other GHGs and (2) the long time it takes for warmth to penetrate into the oceans. Under the aforementioned scenario, the associated sea level rise commitment is much longer term, due to the effects of thermal expansion on sea level. Water has the physical property of expanding as it heats up, therefore, as the warming penetrates deeper into the ocean, an ever-increasing volume of water expands and contributes to ongoing sea level rise. Since it would take centuries for the entire volume of the ocean to warm in response to the effects of GHGs already in the air, sea level rise would continue for centuries. Further glacial melt is also likely.

The 16 climate modelling groups (from 11 countries) contributing to the AR4 produced the most extensive internationally coordinated climate change analysis ever performed. In total, 23 global coupled climate models were used to perform simulations of the 20th century climate, three scenarios of the 21st century (based on low-, medium-, and high-emission scenarios), and three idealized stabilization experiments. Some of the major results include:

- Over the next two decades, all models produce similar warming trends in global surface temperatures, regardless of the scenario. The rate of the projected warming is near 0.2°C/decade, or about twice that of the 'commitment' runs.
- Decadal-average warming over each inhabited continent by 2030 is insensitive to the emission scenario; moreover, the temperature change is very likely to exceed the model generated natural temperature variability by at least a factor of two.
- By the middle of the 21st century the choice of scenario becomes more important for the magnitude of surface warming, and by the end of the 21st century there are clear consequences for which scenario is followed. The best estimate of the global surface temperature change from today to the end of the century is +1.8°C (with a likely range of +1.1°C to +2.9°C) for the low emission scenario (B1, corresponding to a CO_2 equivalent concentration of 600 ppm by 2100) and +4.0°C (+2.4°C to +6.4°C) for the highest emission scenario (A1F1, corresponding to 1550 ppm).
- Geographical patterns of warming show greatest temperature increases at high northern latitudes and over land, with less warming over the southern oceans and North Atlantic, as has been observed in recent decades. In spite of a slowdown of the meridional overturning circulation and changes in the Gulf Stream in the ocean across models, there is still warming over the North Atlantic and Europe due to the overwhelming effects of the increased concentrations of GHGs.
- Snow cover is projected to contract. Widespread increases in thaw depth are projected over most permafrost regions.
- Sea ice coverage is projected to shrink. Large parts of the Arctic Ocean are expected to no longer have year-round ice cover by the middle of the 21st century. In AR4 the results were more suggestive of such changes by the end of the 21st century, but recent changes and new model results suggest that late-summer sea ice could disappear almost completely in just a few decades.
- It is very likely that hot extremes, heat waves, and heavy precipitation events will continue to become more frequent. Models also project a 50–100% decline in the frequency of cold air outbreaks in most regions of the winter NH. Related decreases in frost days contribute to longer growing seasons.
- Projections of sea level rise by the end of the century are similar to previous estimates, ranging from 30 to 40 cm, but do not include possible ice sheet collapse.

• About 60–70% of the projected sea level rise is due to thermal expansion of sea water. There is less certainty of the future contributions from other sources. For instance, the projections include a contribution due to increased ice flow from Greenland and Antarctica at the rates observed over the past decade, but how these flow rates might change in the future is not known.
• Increases in the amount of precipitation are very likely in high latitudes, while decreases are likely in most subtropical land regions, continuing recent trends.
• SLP is projected to increase over the subtropics and middle latitudes, and decrease over high latitudes associated with annular mode changes (NAM/NAO and SAM). Consequently, storm tracks are projected to move poleward, with consequent changes in wind, precipitation, and temperature patterns outside the tropics, continuing the pattern of observed trends over the last few decades.
• Most models warm the central and eastern equatorial Pacific more than the western equatorial Pacific, with a corresponding mean eastward shift in precipitation. ENSO interannual variability is projected to continue in all models, but with large inter-model differences.

The climate models assessed in the AR4 have better and more complete representations of many physical processes, but as our knowledge of the different components of the climate system and their interactions increases, so does the complexity of climate models. Historical changes in land use and changes in the distribution of continental water due to dams and irrigation, for instance, need to be considered. Future projected land cover changes due to human land uses are also likely to significantly affect climate, especially locally, and these effects are only just now being included in climate models.

One of the major advances in climate modelling in recent years has been the introduction of coupled climate-carbon models. Climate change is expected to influence the capacities of the land and oceans to act as repositories for anthropogenic CO_2 and hence provide a feedback to climate change. Although only relatively few global coupled climate models include the complex processes involved with modelling the carbon cycle, this feedback is positive (adding to more warming) in all models so far considered. The addition of carbon cycle feedbacks therefore increases the fraction of anthropogenic emissions that remain in the atmosphere, thereby giving higher values on the warm end of the uncertainty ranges.

2.7 Conclusions

The consequences of the physical changes in climate are addressed extensively in IPCC (2007b). Considerable evidence suggests that recent warming is strongly affecting terrestrial biological systems, including earlier timing of spring events, such as leaf-unfolding, bird migration, and egg-laying, and poleward and upward shifts in ranges in plant and animal species. Moreover, the resilience of many ecosystems is likely to be exceeded this century by an unprecedented combination of climate change, associated disturbances (e.g. flooding, drought, wildfire, insects, and ocean acidification), and other human effects such as land use and change, pollution, and over-exploitation of resources.

An unmistakable sign of climate change, for instance, is the extremely large clusters of dead pine trees from the southern Rockies into vast parts of Canada and Alaska. Forest managers throughout the North American west have called the diebacks 'catastrophic' and 'unprecedented'. The area affected is 50 times larger than the area affected by forest fire with an economic impact nearly five times as great (Logan *et al.*, 2003). The trees are succumbing to the relentless attack of the mountain pine beetle. Warming temperatures have not only removed the natural line of defence against such infestations, namely sufficiently cold temperatures in winter, but they are speeding up the life cycle of the beetle. In contiguous USA, for example, warmer summer temperatures are enabling the beetle to produce two generations in a year, when previously they reproduced once a year (Berg *et al.*, 2006).

Global warming promotes increases in both drought through drying (evaporation) and temperature. With atmospheric temperature increases the water holding capacity goes up at 7%/°C, and has

the effect of drawing moisture out of plants and soils. In many places, even as rains have become heavier (more intense), so too have dry spells become longer. A consequence of more intense but less frequent precipitation events is that what were once 500-year flood events are now more like 30- or 50-year events. After a certain point where the ground is dry and plants have reached wilting point, all of the heat goes into raising temperature and creating heat waves, and then wild fire risk goes up substantially. 'Dry lightning' can then be disastrous, especially in areas where trees are damaged, for example by bark beetles. The risk of wild fire does not necessarily translate into a wild fire if care has been taken in managing the risk by building wild fire breaks, cutting down on litter, and removing diseased and dead trees and vegetation near buildings.

For humans, autonomous adaptation occurs to changing conditions to some degree. Climate change effects occur amidst increases in life expectancy in most places and are thus hard to sort out. Direct effects are nonetheless evident from changes in heat, cold, storms (including hurricanes and tornadoes), drought, and wild fires. The drought-related heat wave in Europe in summer 2003, for instance, killed as many as 55,000 people. On the other hand, fewer cold waves reduce mortality. Safe drinking water is jeopardized by more intense rains and runoff, which can lead to contamination and increased microbial loading. Hence, water-borne diseases have been observed to increase. Also drought and observed earlier snow melt and runoff jeopardize water supplies, especially in summer.

Changes in temperatures, humidity, and precipitation also affect the environment for pests and disease, and have increased risk of certain problems in plants, animals, and humans. Air quality is changing from pollution, and ground level ozone and particulate matter are increasing in most regions, with increased hospital admissions for respiratory disease. Particular human health problems have occurred with spread of West Nile virus, which requires warmer temperatures to survive. Similarly, Lyme disease, borne by ticks, is associated with temperature and precipitation (Chapter 15).

The reality of anthropogenic climate change can no longer be debated. The imperative is to act aggressively to reduce carbon emissions and dependency on fossil fuels, creating instead a sustainable and clean energy future. Mitigation actions taken now mainly have benefits 50 years and beyond because of the huge inertia in the climate system, therefore society will have to adapt to climate change, including its many adverse effects on human health and ecosystems, even if actions are taken to reduce the magnitude and rate of climate change. The projected rate of change far exceeds anything seen in nature in the past 10,000 years and is therefore apt to be disruptive in many ways.

2.8 References

Berg, E.E., Henry, J.D., Fastie, C.L., *et al*. (2006) Spruce beetle outbreaks on the Kenai Peninsula, Alaska, and Kluane National Park and Reserve, Yukon Territory: relationship to summer temperatures and regional differences in disturbance regimes. *Forest Ecology and Management* 227, 219–232.

Delworth, T.L. and Mann, M.E. (2000) Observed and simulated multidecadal variability in the Northern Hemisphere. *Climate Dynamics* 16, 661–676.

Deser, C., Phillips, A.S., and Hurrell, J.W. (2004) Pacific interdecadal climate variability: linkages between the tropics and the north Pacific during boreal winter since 1900. *Journal of Climate* 17, 3109–3124.

Durant, J.M., Stenseth, N.C., Anker-Nilssen, T., *et al*. (2004) Marine birds and climate fluctuation in the North Atlantic. In N.C. Stenseth, G. Ottersen, J.W. Hurrell, and A. Belgrano, eds, *Marine Ecosystems and Climate Variation: The North Atlantic*, pp. 95–105. Oxford University Press, Oxford.

Hawkins, E. and Sutton, R. (2009) The potential to narrow uncertainty in regional climate predictions. *Bulletin of the American Meteorological Society* 90, 1095.

Hoerling, M.P., Hurrell, J.W., Eischeid, J., and Phillips, A. (2006) Detection and attribution of 20th century Northern and Southern African rainfall change. *Journal of Climate* 19, 3989–4008.

Hurrell, J.W. (2002) Recent atmospheric circulation changes and their role in global warming. *FSWX Outlook* 3, 1–10.

Hurrell, J.W., Kushnir, Y., Ottersen, G., and Visbeck, M. (2003) An overview of the North Atlantic oscillation. In J.W. Hurrell, Y. Kushnir, G. Ottersen, and M. Visbeck, eds, *The North Atlantic Oscillation: Climatic Significance and Environmental Impact. Geophysics Monographs*, vol. 134, pp. 1–35. American Geophysical Union, Washington, DC.

Hurrell, J.W. and Deser, C. (2009) Atlantic climate variability. *Journal of Marine Systems*.

IPCC (2007a) The physical science basis. In S. Solomon, *et al.*, eds, *Climate Change 2007*. Cambridge University Press, Cambridge.

IPCC (2007b) Impacts, adaptation and vulnerability. In M.L. Parry, *et al.*, eds, *Climate Change 2007*. Cambridge University Press, Cambridge.

Karl, T.R. and Trenberth, K.E. (2003) Modern global climate change. *Science* 302, 1719–1723.

Kanuscak, P., Hromada, M., Sparks, T.H., and Tryjanowski, P. (2004) Does climate at different scales influence the phenology and phenotype of the river warbler *Locustella fluviatilis*? *Oecologia* 141, 158–163.

Knight, J.R., Allan, R.J., Folland, C.K., *et al*. (2005) A signature of persistent natural thermohaline circulation cycles in observed climate. *Geophysical Research Letters* 32, L20708.

Logan, J.A., Regniere, J., and Powell, J.A. (2003) Assessing the impacts of global warming on forest pest dynamics. *Frontiers in Ecology and the Environment* 1, 130–137.

Marshall, G.J. (2003) Trends in the southern annular mode from observations and reanalyses. *Journal of Climate* 16, 4134–4143.

Mysterud, A., Stenseth, N.C., Yoccoz, N.G., *et al*. (2003) The response of terrestrial ecosystems to climate variability associated with the North Atlantic oscillation. In J.W. Hurrell, Y. Kushnir, G. Ottersen, and M. Visbeck, eds, *The North Atlantic Oscillation: Climatic Significance and Environmental Impact. Geophysics Monographs*, vol. 134, pp. 235–262. American Geophysical Union, Washington, DC.

Quadrelli, R. and Wallace, J.M. (2004) A simplified linear framework for interpreting patterns of Northern Hemisphere wintertime climate variability. *Journal of Climate* 17, 3728–3744.

Rosenzweig, C., Karoly D., Vicarelli, M., *et al.* (2008) Attributing physical and biological impacts to anthropogenic climate change. *Nature* 453, 353–358.

Schneider, A., Friedl, M.A., and Potere, D. (2009) A new map of global urban extent from MODIS satellite data. *Environmental Research Letters* 4, 044003.

Seager, R., Kushnir, Y., Ting, M., *et al*. (2008) Would advance knowledge of 1930s SSTs have allowed prediction of the dust bowl drought? *Journal of Climate* 21, 3261–3281.

Stenseth, N.C., Ottersen, G., Hurrell, J.W., and Belgrano, A. (2005) *Marine Ecosystems and Climate Variation*. Oxford University Press, Oxford.

Stevens, B. and Feingold, G. (2009) Untangling aerosol effects on clouds and precipitation in a buffered system. *Nature* 461, 607–613.

Thompson, D.W.J. and Wallace, J.M. (2000) Annular modes in the extratropical circulation. Part I, Month-to-month variability. *Journal of Climate* 13, 1000–1016.

Trenberth K.E. (1997) The use and abuse of climate models in climate change research. *Nature* 386, 131–133.

Trenberth, K.E. (2007) Warmer oceans, stronger hurricanes. *Scientific American* July, 45–51.

Trenberth, K.E. and Caron, J.M. (2000) The southern oscillation revisited: sea level pressures, surface temperatures and precipitation. *Journal of Climate* 13, 4358–4365.

Trenberth, K.E. and Hurrell, J.W. (1994) Decadal atmosphere–ocean variations in the Pacific. *Climate Dynamics* 9, 303–319.

Trenberth, K.E. and Paolino, D.A. (1980) The Northern Hemisphere sea level pressure data set: trends, errors and discontinuities. *Monthly Weather Review* 108, 855–872.

Trenberth, K.E. and Shea, D.J. (2006) Atlantic hurricanes and natural variability in 2005. *Geophysics Research Letters* 33, L12704.

Trenberth, K.E., Stepaniak, D.P., and Smith, L. (2005) Interannual variability of patterns of atmospheric mass distribution. *Journal of Climate* 18, 2812–2825.

Webster, P.J., Holland, G.J., Curry, J.A., and Chang, H.-R. (2005) Changes in tropical cyclone number, duration and intensity in a warming environment. *Science* 309, 1844–1846.